



The Electrochemical Detection of Alizarin Red at Electrofabricated CeO₂-Reduced Graphene Oxide Nanostructures

 Neslihan ÇELEBİ^{1,2,*},  Emir COŞKUN²

¹ Department of Chemistry and Chemical Processing Technologies, Erzurum Vocational College, Atatürk University, Erzurum, Turkey

² Department of Nanoscience and Nanoengineering, Ataturk University, Erzurum, Turkey

* Corresponding author E-mail: nes25@atauni.edu.tr

ARTICLE INFO

Received : 11.28.2024

Accepted : 03.09.2025

Published : 07.15.2025

Keywords:

Alizarin Red

Cerium Oxide

Electrochemical Deposition

Reduced Graphene Oxide

ABSTRACT

Cerium oxide-reduced graphene oxide (CeO₂-rGO) nanostructures were successfully fabricated on indium tin oxide (ITO) electrode surface using one-pot electrochemical technique. The prepared nanostructures and modified surfaces (CeO₂-rGO/ITO) were investigated for the electrochemical determination of Alizarin red (AR). Firstly, electrocatalytic activities of different modified surfaces were compared by cyclic voltammograms (CVs). For further analysis, concentration-dependent measurements were recorded using differential pulse voltammetry (DPV). The detection limit of AR on the CeO₂-rGO/ITO electrode was calculated as 1.9 µM. The modified surface was successfully used to detect AR, which may add a new dimension to the detection of Alizarin derivatives materials.

Contents

1. Introduction	28
2. Experimental Method	29
3. Results and discussion	29
3.1. Characterization of CeO ₂ -rGO nanostructures	29
3.2. Electrochemical detection of AR on CeO ₂ -rGO	30
4. Conclusions	30
Acknowledgments	31
Conflict of Interest	31
Funding	31
References	31

1. Introduction

Water is vital to humans and all living things as the primary substance of life. Although 71% of the world is covered with water, only 2.5% is available as fresh water [1]. Only 0.27% of the available freshwater is accessible; the rest is underground, swamps, and frozen polar ice caps [2]. In recent years, inadequate access to clean drinking water has become a significant problem worldwide due to industrialization, rapid population growth, environmental pollution, climate change, and prolonged droughts [3]. Water resources are constantly polluted by various toxic substances, including dyes, heavy metal ions, oils, and other

chemicals released from multiple industries [4]. Dyes and pigments are widely used in the leather, plastic, textile, cosmetics, paper, silk, food, and dyeing industries [5].

While the dye wastewater of the textile industry contains the highest amount of dye (54%), dyeing, pulp and paper production, and paint industries also release high amounts of dye wastewater into the environment [6]. Dyes are not biodegradable and have a stable chemical structure, which makes them resistant to fading when exposed to light, heat, and oxidizing agents [7]. They also adversely affect living beings due to their teratogenic, carcinogenic, and mutagenic properties. Azo dyes are the largest and most versatile class of organic dyes [6]. They contain one or more azo bonds (–

Cite this article Çelebi N, Coşkun E. The Electrochemical Detection of Alizarin Red at Electrofabricated CeO₂-Reduced Graphene Oxide Nanostructures. *International Journal of Innovative Research and Reviews (INJIRR)* (2025) 9(1) 28-31

Link to this article: <http://www.injirr.com/article/view/239>



Copyright © 2025 Authors.

This is an open access article distributed under the [Creative Commons Attribution-NonCommercial-NoDerivatives 4.0 International License](https://creativecommons.org/licenses/by-nc-nd/4.0/), which permits unrestricted use, and sharing of this material in any medium, provided the original work is not modified or used for commercial purposes.

N = N-) as a chromophore group in conjunction with aromatic structures. They include functional groups such as -OH and -SO₃H [8]. The complex aromatic structures of azo dyes make them more stable and difficult to remove from wastewater discharged into water bodies [9].

Considering that dyes are toxic and carcinogenic, removing synthetic dyes from wastewater constitutes an essential area of work regarding health and safety. Many different techniques, such as precipitation, ion exchange, electrochemical, photochemical, photoelectrochemical, electrocoagulation, and adsorption, are used to remove polluting dyes from aqueous media [10]. However, these procedures have their limitations. Therefore, advanced oxidation processes (AOPs) developed in the last decade are successfully applied to remove dyes in aqueous systems [11].

Alizarin red (AR) is an anthraquinone dye widely used in the textile industry. Anthraquinone dyes are compounds containing aromatic rings, which do not naturally decompose due to their complex structures [12]. Therefore, they are toxic to biota and aquatic environments. AR can cause toxic effects on humans, such as skin and eye irritation, severe headaches, and irregular lung function [13].

Cerium oxide (CeO₂) has been extensively investigated due to its energy reserves, outstanding oxygen storage capacity, and extraordinary ability to facilitate catalytic reactions efficiently [14]. Furthermore, CeO₂, as a rare earth metal, has attracted significant attention due to its high activity, low cost, and environmentally friendly properties [15, 16]. Numerous studies have observed the high capacitance performance and improved stability of CeO₂/reduced graphene oxide (rGO) nanocomposites. Many researchers attribute this impressive performance to the synergistic effect of rGO and CeO₂. Considering that the surface morphology of CeO₂ significantly affects its reactivity, there is significant potential to improve the material synthesis process to customize the morphology of CeO₂ for improved activity. Li and Liu [17] have demonstrated enhanced electrochemical properties by immobilizing CeO₂ with rGO. CeO₂ NPs immobilized along the graphene matrix can complement each other, overcoming the restackability of graphene and the low conductivity of CeO₂. CeO₂ nanostructures are also used in sensor technologies due to their high specific surface areas, practical electrochemical activities, and ability to facilitate electron transfer processes with reduced overpotential [18–20].

This study discussed in detail the usability of an extraordinary, new removal agent for the removal of water-soluble AR from water. Besides, the use of composite material containing CeO₂/rGO nanostructures in the electrochemical removal of AR was introduced to the literature.

2. Experimental Method

Cerium (III) nitrate (Ce(NO₃)₃), graphene oxide (GO), potassium nitrate (KNO₃), sodium phosphate dibasic (Na₂HPO₄), and Alizarin red (AR) were supplied by Sigma and used as received. All electrochemical experiments were carried out in a three-electrode cell system. Pt wire was selected as the counter electrode and Ag/AgCl as the

reference electrode. An indium tin oxide (ITO) electrode was used as the working electrode for the electrochemical synthesis of CeO₂-rGO nanostructures. For one-pot synthesis, 10 mM Ce(NO₃)₃ and GO (in 0.1 M KNO₃) were mixed 1:1 and deposited at a constant potential of -1.2 V for 15 minutes. Field emission scanning electron microscopy (FESEM) and Energy Dispersive X-ray spectroscopy (EDS) were used to characterize the produced CeO₂-rGO nanostructures. For the electrochemical determination of AR, 0.1 M phosphate buffer (pH=6.5) containing 1 mM AR was prepared. Cyclic voltammograms (CVs) and differential pulse voltammograms (DPVs) were performed with a BAS100i model potentiostat. Voltammetric measurements were recorded at a scan rate of 50 mV/s in the potential window from -1 V to +1.2 V.

3. Results and discussion

3.1. Characterization of CeO₂-rGO nanostructures

The characterization of CeO₂-rGO nanostructures has been studied and reported in detail by our research group in previous reports [21]. Figure 1.a displays the XRD spectrum of CeO₂-rGO nanostructures on the ITO electrode surface, showing diffraction peaks for ITO, CeO₂, and rGO. Because of the thin film deposition, ITO peaks also appear in the spectrum. CeO₂ peaks occur at 28.42° (111), 32.95° (200), 47.30° (220), 56.34° (311), 59.09° (222), 69.34° (400), and 76.60° (331) degrees, consistent with JCPDS card no: 34-0394. The rGO peak appears as a broad peak near 26.5° degrees. This spectrum confirms that the CeO₂-rGO nanostructures, produced by electrochemical methods, are crystalline.

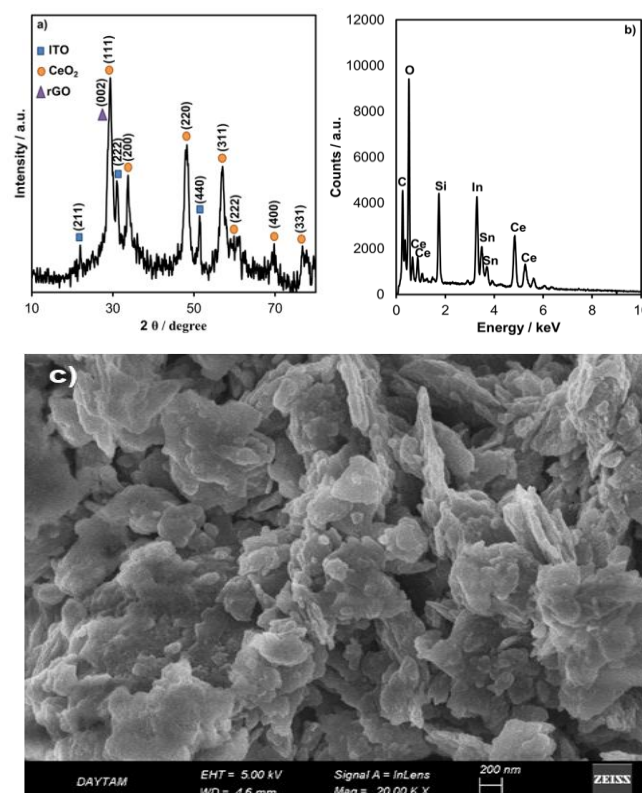


Figure 1 XRD pattern (a), EDS spectra (b), and FESEM image (c) of CeO₂-rGO nanostructures

Morphological characterization was investigated using the FESEM technique (Figure 1.b). It was found that CeO₂-rGO nanostructures completely covered the ITO substrate surface and showed growth in the form of nanoparticles. Structural characterization was done via the EDS technique (Figure 1.c). It was observed that CeO₂-rGO nanostructures were composed of Ce, O, and C elements. In addition, the atomic ratios of Ce, O, and C elements were determined as 10.21%, 48.29%, and 41.49%, respectively.

3.2. Electrochemical detection of AR on CeO₂-rGO

The electrochemical determination of AR was studied using CV analysis. First, the electrocatalytic activities of bare ITO, CeO₂/ITO, and CeO₂-rGO/ITO electrodes were compared in the electrolyte containing 1 mM AR in 0.1 M PBS buffer (pH = 6.5) (Figure 2.a). As seen in the CV curves in Figure 2.a, the unmodified ITO electrode exhibited a current that was invisibly small for AR determination. When the ITO surface was coated with CeO₂ nanostructures, the AR sensing response of the electrode was observed (Figure 2.a, inset graph). In addition, the presence of CeO₂-rGO nanostructures on the ITO surface exhibited a higher current for AR determination at the same concentration. The AR oxidation current of the CeO₂-rGO/ITO electrode was 265 μ A, which was approximately 10 times that of CeO₂/ITO. An irreversible oxidation peak was detected in the CV plot of the CeO₂-rGO/ITO electrode, starting at +400 mV and reaching a maximum of approximately +700 mV. This irreversible oxidation peak is known to correspond to the oxidation of anthraquinone or ortho-quinone moiety. Moreover, this potential value is consistent with that reported in the literature for the redox reaction of anthraquinone [22].

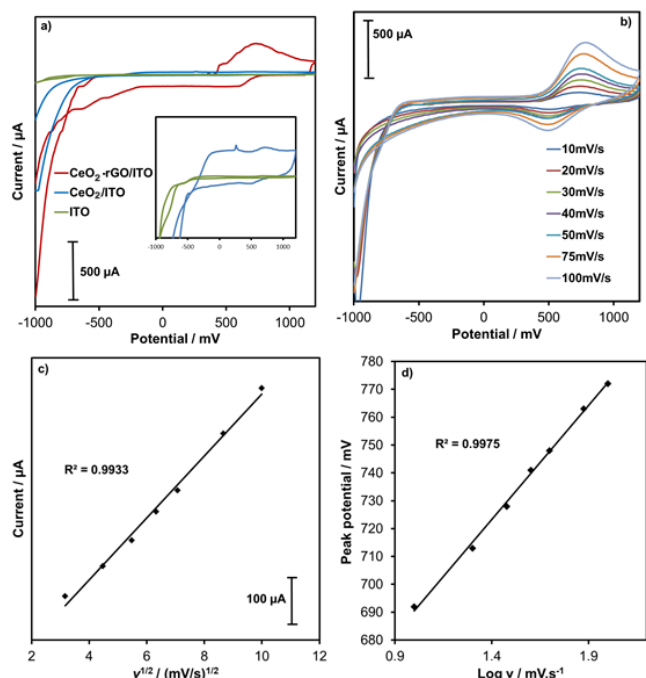


Figure 2 CVs of ITO, CeO₂/ITO, and CeO₂-rGO/ITO electrodes (a) in 1 mM AR solution. CV curves of various scan rates (b), square root of scan rate-current (c), $\log v$ -peak potential graph (d) for CeO₂-rGO/ITO electrode.

To determine the AR oxidation kinetics on the CeO₂-rGO/ITO electrode surface, CV graphs were recorded at various scan speeds ranging from 10 mV/s to 100 mV/s (Figure 2.b). It was determined that the oxidation peak

current of AR increased with the increase in scan speed. The current graph against the square root of the scan speed was plotted using the CV curves in Figure 2.c. The fact that the graph given in Figure 2.c is a linear indicates that AR on the CeO₂-rGO surface is oxidized via a diffusion-controlled mechanism. Moreover, the fact that the graph of the peak potential versus $\log v$ is also a linear and the electron transfer coefficient ($\alpha=0.35$) calculated using the slope of this line supported that AR was oxidized quasi-irreversibly.

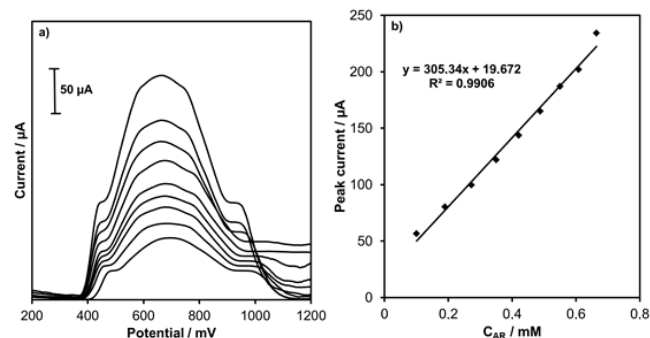


Figure 3 DPVs of CeO₂-rGO/ITO electrode for various concentrations (a) and calibration curve (b).

DPV plots were recorded for different concentrations to study the effect of AR concentration (Figure 3.a). The current value exhibited by the electrode also increased with increasing concentration. The concentration-current plot (calibration curve) was obtained using DPV plots (Figure 3.b). Limit of detection (LOD) value was calculated from the calibration curve as 1.9 μ M. The comparison of these values with the electrodes available in the literature is summarized in Table 1. CeO₂-rGO/ITO electrode exhibited properties comparable to those in the literature for the determination of AR.

Table 1 Comparison of some electrode materials for the determination of AR.

Electrode	Linear Range (μ M)	LOD (μ M)	Ref.
TX-100MCNTPE	2–10	1000	[23]
GCE/Sa(DODAB) _{0.25}	0.01–0.1	0.0038	[24]
DA/pAPBA/RGO/GCE	0.090–10	0.022	[25]
PLMCPE	1.5–3.5	0.68	[26]
CeO ₂ -rGO/ITO	100–700	1.9	This work

TX-100MCNTPE: TX-100 modified carbon nanotube paste electrode, GCE: Glassy carbon electrode, DODAB: dimethyldioctadecylammonium bromide, DA: Dopamine, pAPBA: poly(3-aminophenylboronic acid), rGO: reduced graphene oxide, PLMCPE: poly leucine modified carbon paste electrode.

4. Conclusions

In this study, CeO₂-rGO nanocomposites were produced on the ITO electrode surface by a one-pot electrochemical synthesis method. The characterizations showed that the nanocomposite was successfully prepared in the desired form. Moreover, CeO₂-rGO electrodes were investigated in the electrochemical determination of AR. The electrochemical behavior of AR was analyzed using the CV technique. The detection limit of AR on the CeO₂-rGO/ITO electrode was calculated as 1.9 μ M based on the DPV technique. The modified surface was successfully used to detect AR, which can add a new dimension to the detection of Alizarin derivative materials.

Acknowledgments

The authors thank Atatürk University Eastern Anatolia High Technology and Research Center (DAYTAM) for supporting their work characterizing the synthesized electrodes. The authors would like to thank Dr. Hülya Öztürk Doğan for her support in electrochemical measurements.

Conflict of Interest

Author declares that they do not have any conflict of interest.

Funding

None.

References

- [1] Musie W, Gonfa G. Fresh water resource, scarcity, water salinity challenges and possible remedies: A review'. *Heliyon* (2023) **9**(8):18685. doi:10.1016/j.heliyon.2023.e18685.
- [2] Cavin L. *1 - Freshwater Environments and Fishes*, in *Freshwater Fishes: 250 Million Years of Evolutionary History*; Elsevier (2017). 1–14.
- [3] Ahmed T, Zounemat-Kermani M, Scholz M. Climate Change, Water Quality and Water-Related Challenges: A Review with Focus on Pakistan'. *Int J Environ Res Public Health* (2020) **17**(22):8518. doi:10.3390/ijerph17228518.
- [4] Wang J, Azam W. Natural resource scarcity, fossil fuel energy consumption, and total greenhouse gas emissions in top emitting countries'. *Geoscience Frontiers* (2024) **15**(2):101757. doi:10.1016/j.gsf.2023.101757.
- [5] Karimi-Maleh H. Recent advances in carbon nanomaterials-based electrochemical sensors for food azo dyes detection'. *Food and Chemical Toxicology* (2022) **164**:112961. doi:10.1016/j.fct.2022.112961.
- [6] Singh S, Patidar R, Srivastava VC, Lo S-L, Nidheesh PV. A critical review on the degradation mechanism of textile effluent during electrocatalytic oxidation: Removal optimization and degradation pathways'. *Journal of Environmental Chemical Engineering* (2023) **11**(6):111277. doi:10.1016/j.jece.2023.111277.
- [7] Venkatesh S, Arutchelvan V. Biosorption of Alizarin Red dye onto immobilized biomass of *Canna indica*: isotherm, kinetics, and thermodynamic studies'. *Desalination and Water Treatment* (2020) **196**:409–421. doi:10.5004/dwt.2020.25798.
- [8] Bessegato GG, Brugnera MF, Zanoni M. Electroanalytical sensing of dyes and colorants'. *Current Opinion in Electrochemistry* (2019) **16**:134–142. doi:10.1016/j.coelec.2019.05.008.
- [9] Ali H. Biodegradation of Synthetic Dyes—A Review'. *Water Air Soil Pollut* (2010) **213**(1):251–273. doi:10.1007/s11270-010-0382-4.
- [10] Singh S, Srivastava VC, Mall ID. Mechanism of Dye Degradation during Electrochemical Treatment'. *J. Phys. Chem. C* (2013) **117**(29):15229–15240. doi:10.1021/jp405289f.
- [11] Moreira FC, Boaventura R, Brillas E, Vilar V. Electrochemical advanced oxidation processes: A review on their application to synthetic and real wastewaters'. *Applied Catalysis B: Environmental* (2017) **202**:217–261. doi:10.1016/j.apcatb.2016.08.037.
- [12] Panizza M, Oturan MA. Degradation of Alizarin Red by electro-Fenton process using a graphite-felt cathode'. *Electrochimica Acta* (2011) **56**(20):7084–7087. doi:10.1016/j.electacta.2011.05.105.
- [13] Zhang J, Chi Y, Feng L. The mechanism of degradation of alizarin red by a white-rot fungus *Trametes gibbosa*'. *BMC Biotechnol* (2021) **21**:64. doi:10.1186/s12896-021-00720-8.
- [14] Nosrati H, Heydari M, Khodaei M. Cerium oxide nanoparticles: Synthesis methods and applications in wound healing'. *Materials Today Bio* (2023) **23**:100823. doi:10.1016/j.mtbio.2023.100823.
- [15] Ahmed HE. Green Synthesis of CeO₂ Nanoparticles from the *Abelmoschus esculentus* Extract: Evaluation of Antioxidant, Anticancer, Antibacterial, and Wound-Healing Activities'. *Molecules* (2021) **26**(15, Art. no. 15). doi:10.3390/molecules26154659.
- [16] Durmuş S, Dalmaz A, Özdiğer M, Sivrikaya S. Preparation of Cerium Oxide Nanoparticles: An Efficient Catalyst to the Synthesis of Dimeric Disulphide Schiff Bases'. *CBUJOS* (2017) **13**(1, Art. no. 1). doi:10.18466/cbayarfe.282116.
- [17] Li T, Liu H. A simple synthesis method of nanocrystals CeO₂ modified rGO composites as electrode materials for supercapacitors with long time cycling stability'. *Powder Technology* (2018) **327**:275–281. doi:10.1016/j.powtec.2017.12.073.
- [18] Ahmed J, Faisal M, Algethami JS, Alsaiani M, Jalalah M, Harraz FA. CeO₂-ZnO@biomass-derived carbon nanocomposite-based electrochemical sensor for efficient detection of ascorbic acid'. *Analytical Biochemistry* (2024) **692**:115574. doi:10.1016/j.ab.2024.115574.
- [19] Ahmed J, Faisal M, Algethami JS, Alkorbi AS, Harraz FA. Facile synthesis of CeO₂-CuO-decorated biomass-derived carbon nanocomposite for sensitive detection of catechol by electrochemical technique'. *Materials Science in Semiconductor Processing* (2024) **172**:108098. doi:10.1016/j.mssp.2023.108098.
- [20] Wang W, Xu W, Zhao Z, Cheng M, Xun M, Liu H. Method and Application of Surface Modification of Cerium Dioxide'. *Advanced Engineering Materials* (2024) **26**(14):2400092. doi:10.1002/adem.202400092.
- [21] Çelebi N, Temur E, Doğan H, Yüksel A. The electrochemical fabrication of Cu@CeO₂-rGO electrode for high-performance electrochemical nitrite sensor'. *Diamond and Related Materials* (2024) **143**:110907. doi:10.1016/j.diamond.2024.110907.
- [22] Schumacher S, Nagel T, Scheller FW, Gajovic-Eichmann N. Alizarin Red S as an electrochemical indicator for saccharide recognition'. *Electrochimica Acta* (2011) **56**(19):6607–6611. doi:10.1016/j.electacta.2011.04.081.
- [23] Monnappa A, Manjunatha JG, Bhatt AS, Chenthatil R, Ananda P. Electrochemical Sensor for the Determination of Alizarin Red-S at Non-ionic Surfactant Modified Carbon Nanotube Paste Electrode'. *Physical Chemistry Research* (2019) **7**(3):523–533. doi:10.22036/pcr.2019.185875.1636.
- [24] Deffo G, Temgoua R, Mbokou S, Njanja E, Tonlé I, Ngameni E. A sensitive voltammetric analysis and detection of Alizarin Red S onto a glassy carbon electrode modified by an organosmectite'. *Sensors International* (2021) **2**:100126. doi:10.1016/j.sintl.2021.100126.
- [25] Liu F, Kan X. Dual-analyte electrochemical sensor for fructose and alizarin red S specifically sensitive detection based on indicator displacement assay'. *Electrochimica Acta* (2019) **319**:286–292. doi:10.1016/j.electacta.2019.07.001.
- [26] Mouly KP, Manjunatha JG, Osman SM, Ataollahi N. A novel and efficient voltammetric sensor for the simultaneous determination of alizarin red S and tartrazine by using poly(leucine) functionalized carbon paste electrode'. *Journal of Environmental Science and Health, Part A* (2024) **59**(3):103–112. doi:10.1080/10934529.2024.2339160.